Journal of Theoretical Biology 329 (2013) 20–31

Contents lists available at SciVerse ScienceDirect

Journal of Theoretical Biology

journal homepage: www.elsevier.com/locate/yjtbi

Modeling low-dose mortality and disease incubation period of inhalational anthrax in the rabbit ☆

Bradford W. Gutting [a,*], David Marchette [d], Robert Sherwood [b], George A. Andrews [a], Alison Director-Myska [c], Stephen R. Channel [c], Daniel Wolfe [c], Alan E. Berger [a,1], Ryan S. Mackie [a], Brent J. Watson [a], Andrey Rukhin [d]

[a] CBR Concepts and Experimentation Branch (Z21), Naval Surface Warfare Center, Dahlgren Division, Dahlgren, VA, USA
[b] Lovelace Respiratory Research Institute, Albuquerque, NM, USA
[c] Defense Threat Reduction Agency, Fr. Belvoir, MD, USA
[d] Sensor Fusion Branch (Q33), Naval Surface Warfare Center, Dahlgren Division, Dahlgren, VA, USA

HIGHLIGHTS

- Data were collected from NZW rabbits exposed to high doses of *B. anthracis* Ames spore aerosols.
- The data were modeled using the Competing Risks model of inhalational anthrax.
- The low dose-response (lethality) extrapolation data agreed with known dose–response data.
- The model predicted a 14.5 h median low-dose germination period.
- The model predicted a low-dose disease incubation period between 14.7 and 16.8 days.

ARTICLE INFO

Article history:
Received 26 October 2012
Received in revised form
14 March 2013
Accepted 21 March 2013
Available online 6 April 2013

Keywords:
Inhalational anthrax
Ames
Rabbit
Stochastic model
Dose–response

ABSTRACT

There is a need to advance our ability to conduct credible human risk assessments for inhalational anthrax associated with exposure to a low number of bacteria. Combining animal data with computational models of disease will be central in the low-dose and cross-species extrapolations required in achieving this goal. The objective of the current work was to apply and advance the competing risks (CR) computational model of inhalational anthrax where data was collected from NZW rabbits exposed to aerosols of Ames strain *Bacillus anthracis*.

An initial aim was to parameterize the CR model using high-dose rabbit data and then conduct a low-dose extrapolation. The CR low-dose attack rate was then compared against known low-dose rabbit data as well as the low-dose curve obtained when the entire rabbit dose–response data set was fitted to an exponential dose–response (EDR) model. The CR model predictions demonstrated excellent agreement with actual low-dose rabbit data. We next used a modified CR model (MCR) to examine disease incubation period (the time to reach a fever $>40\ ^{\circ}C$). The MCR model predicted a germination period of 14.5 h following exposure to a low spore dose, which was confirmed by monitoring spore germination in the rabbit lung using PCR, and predicted a low-dose disease incubation period in the rabbit between 14.7 and 16.8 days.

Overall, the CR and MCR model appeared to describe rabbit inhalational anthrax well. These results are discussed in the context of conducting laboratory studies in other relevant animal models, combining the CR/MCR model with other computation models of inhalational anthrax, and using the resulting information towards extrapolating a low-dose response prediction for man.

Published by Elsevier Ltd.

1. Introduction

Inhalational anthrax is caused by inhalation of *Bacillus anthracis* spores (Frazier *et al.*, 2006; Mock and Fouet, 2001; Canter, 2005; Dixon *et al.*, 1999). The use of *B. anthracis* spores as a bioweapon was demonstrated in the fall of 2001 when spore-laced letters were sent through the US mail system causing five inhalational

* Corresponding author. Tel.: +1 540 653 0438.
E-mail addresses: bradford.gutting@navy.mil, DLGR_NSWC_Z20@navy.mil (B.W. Gutting).
[1] Current address: Lowe Family Genomics Core, Johns Hopkins University School of Medicine, Baltimore, MD, USA.
☆This work was supported by the Defense Threat Reduction Agency (BA06TAS022).

0022-5193/$ - see front matter Published by Elsevier Ltd.
http://dx.doi.org/10.1016/j.jtbi.2013.03.020

anthrax fatalities (Holtz *et al.*, 2003; Jernigan *et al.*, 2002; Dewan *et al.*, 2002). Today, *B. anthracis* may represent the single greatest biological warfare threat (MacIntyre *et al.*, 2006).

An important component in preparedness planning for inhalational anthrax is developing a better understanding of the risk of disease for a given spore dose exposure, particularly in the low-dose range (Raber, 2011; Coleman *et al.*, 2008; Bartrand *et al.*, 2008). While it is generally accepted that there is a high risk of disease associated with exposure to a high spore dose, the risk of disease associated with low-dose exposure is poorly understood. This uncertainty was highlighted in the wake of the 2001 anthrax attacks, where decision makers adopted a 'no growth' policy for building decontamination and re-occupancy (Canter, 2005; Raber, 2011; Coleman *et al.*, 2008), which was essentially a zero-tolerance policy for exposure to a single *B. anthracis* spore. The reasons for the uncertainty are many, but it is clear that a significant contributor is the fact that naturally occurring inhalational anthrax in man is exceptionally rare (Frazier *et al.*, 2006; Watson and Keir, 1994; Hambleton *et al.*, 1994). As a result, the amount of human data that can be directly used to support human risk assessment is limited. It follows, therefore, that human dose–response predictions will have to be extrapolated from relevant inhalational anthrax animal models and, as noted in a recent review, successful extrapolation of animal data will require advancement of both biological and computational dose–response models (Raber, 2011).

The objective with the current work was to collect data from the NZW rabbit model of inhalation anthrax to examine and advance the competing risk (CR) model of inhalational anthrax. The work focused on modeling dose–response, spore germination, and disease incubation period. The competing risk model of inhalational anthrax was originally developed by Brookmeyer *et al.* (2001) and Brookmeyer and Blades (2002) and then advanced by Wilkening (2006) and Wilkening (2008) and used non-human primate (NHP) data as well as human data collected from the Sverdlovsk outbreak in Russia. The authors concluded the model's attack rate and incubation period were consistent with the NHP and human data. For this reason, we aimed to examine the model in a second species, the NZW rabbit model of inhalation anthrax. The NZW rabbit is a widely used animal model for inhalational anthrax natural history studies and because rabbits are fully protected with the human anthrax vaccine, they are also used for vaccine efficacy studies (Coleman *et al.*, 2008; Pitt *et al.*, 2001; Zaucha *et al.*, 1998; EPA, 2011; Yee *et al.*, 2010; Gutting *et al.*, 2008; Twenhafel, 2011; Gutting *et al.*, 2012). As discussed below, rabbits in the current work were exposed in pairs (one naïve, one vaccinated) and the aim was to monitor disease in groups of rabbits where bacteria were able to escape, replicate, and cause death (naïve animals) and directly compare those observations side-by-side with an equally-dosed vaccinated group where bacterial outgrowth and disease was prevented. In addition to providing useful information on the host–pathogen interaction in immunized animals, the vaccine group served as an important control group for the naive animal response.

2. Methods and Materials

2.1. Competing risks (CR) and modified competing risks (MCR) model

2.1.1. Competing risks (CR) model: attack rate (dose–response)

Our first aim was to examine the rabbit attack rate using the CR model as described by Brookmeyer *et al.* (2003, 2005). The mathematical model is built on the premise that a *B. anthracis* spore will meet one of two fates: the spore will either be removed (i.e., cleared) and thereby incapable of contributing to disease; or it will germinate, become metabolically active and thereby cause disease. In this model, clearance is the removal of the infective spore particle and no distinction is made among the different mechanisms the host uses to eliminate spores: i.e., mucociliated, immune-mediated, or any other host clearance process. An estimate of the clearance rate is obtained by measuring the decrease in observable spores in the animal lungs over time (see below). The CR model describes the dynamics (i.e., competition) between these two processes. Let the clearance rate θ represent the hazard rate or risk per unit time that a deposited spore (that has not previously germinated or been cleared) will be cleared from the lung, and let λ represent the hazard rate or risk per unit time that a deposited spore will germinate. In this model, both θ and λ are assumed to be independent of the elapsed time after inhalation and independent of the number of spores. The probability density functions for germination time, t_1, and clearance time, t_2, respectively, are

$$\lambda e^{-\lambda t_1} \text{ and } \theta e^{-\theta t_2} \tag{1}$$

Viewed as independent exponential processes, the joint probability density function for germination and clearance times is the product of the two individual density functions in Eq. (1),

$$\lambda e^{-\lambda t_1}\ \theta e^{-\theta t_2} \tag{2}$$

and the probability $p=p(\lambda,\theta)$ that an individual spore germinates before it is cleared is the integral of the joint probability density function over the region $0\le t_1\le t_2$, which, after integrating the expression in Eq. (2) over t_2 in (t_1,∞), is

$$\int_0^\infty \lambda e^{-\lambda t_1} e^{-\theta t_1}\, dt_1 = \frac{\lambda}{\lambda+\theta} \tag{3}$$

If an individual is exposed to D spores, and the competing processes of germination and clearance of each spore are independent, then the probability that 1 or more spores germinate is $1-b(0;D,p)$, where $b(x;D,p)$ is the binomial distribution probability that exactly x "successes" occur out of D independent trials when the probability of success in any one trial is p given by Eq. (3). Now

$$b(x,D,p)=\binom{D}{x}p^x(1-p)^{D-x}=\frac{D!}{(D-x)!x!}p^x(1-p)^{D-x} \tag{4}$$

and as noted in Brookmeyer *et al.* (2005), if $\lambda \ll \theta$ (which is indeed the case for *B. anthracis*, cf. the data herein and in Brookmeyer *et al.* (2005), in which case p is small, then $b(0;D,p)$ is well approximated by the Poisson distribution value $p(0;\mu=Dp)=e^{-Dp}$. One way to see this is to observe that $b(0;D,p)=(1-p)^D$, so $\ln b(0;D,p)=D\ln(1-p)$, and using a Taylor expansion for $\ln(1-p)$ for p near 0 gives:

$$\ln b\ (0;\ D,\ p) = D[-p-p^2/2-p^3/3\ldots] \tag{5}$$

If the expression on the right is well approximated by $-Dp$, then $b(0;D,p)$ is well approximated by $\exp(-Dp)$, so the probability, π, that an individual exposed to a dose, D, of spores gets anthrax is well approximated by

$$\pi=\pi(D)=1-\exp(-Dp)=1-\exp\left(\frac{-D\lambda}{\lambda+\theta}\right) \tag{6}$$

The attack rate for disease, in this case lethality, given by Eq. (6) is the dose–response relationship that was found to be consistent when NHP data was used to model human data obtained from the Sverdlovsk outbreak (Brookmeyer *et al.*, 2005; Henderson *et al.*, 1956). This is the dose–response relationship we aimed to test in the initial aspects of the current work using the rabbit model of inhalational anthrax. We derived the clearance and germination rates in the rabbit following high, lethal-dose exposures to Ames spore aerosols and then used these parameter values with Eq. (6) to produce a theoretical low-dose–response curve. We then collated all known low-dose–response data that has been collected in the

rabbit (to our knowledge), in which groups of rabbits were exposed to Ames spore aerosols, and compared the laboratory observations with the model predictions. For analyzing groups of rabbits exposed to a mean dose, D, of spores, the probability of observing x deaths in N exposed rabbits was modeled by the binomial distribution probabilities $b(x;N,\pi)$, where π is determined from Eq. (6).

2.1.2. Exponential dose–response (EDR) model fit

For comparison, the entire rabbit dose–response data set was fit to an exponential dose response (EDR) model [$\pi(D)=1-\exp(-kD)$]. The EDR model was shown by Bartrand *et al.* (2008) to fit inhalational anthrax dose–response data collected in NHPs and guinea pigs. As described by Bartrand *et al.* (2008), the dose–response parameter, k, was estimated using *R* statistical computing language software using the Broyden–Fletcher–Goldfarb–Shanno (BFGS) algorithm and the maximum likelihood estimation (MLE) minimization method.

2.1.3. Competing risks (CR) model: spore germination period

Brookmeyer *et al.* (2005) also derived an expression for the disease incubation period. Here, it was assumed that clinical symptoms occurred immediately following spore germination. That is, there was no time delay built into the model to account for the time required for newly germinated spores to replicate and secrete toxins. Brookmeyer *et al.* (2005) extended the competing risks model by employing an exponentially distributed lag phase, as discussed in the Supplemental Material S2. Under the assumption that symptoms occur immediately following germination, the model is actually describing the germination period and not the disease incubation period. Given this, it follows that the probability, $p(t)$, that a given spore will germinate before it is cleared (i.e., that the spore will cause infection) and that germination will happen at some time between 0 and t, is the area under the joint probability function in Eq. (2) over the region $\{0<t_1<t_2\}\cap\{0<\cap\ t_1<t\}$, which is

$$\left(\frac{\lambda}{\lambda+\theta}\right)(1-e^{-(\lambda+\theta)t}) \tag{7}$$

Using the assumption that $\lambda \ll \theta$, in which case $p(t)$ given by Eq. (7) will be small, the probability, $F(t)$, that at least one spore germinates between time 0 and time t after a dose of D spores is

$$F(t)=1-b(0;\ D,\ p)\approx 1-\exp(-Dp)=1-\exp\left[\frac{-D\lambda}{\lambda+\theta}(1-e^{-(\lambda+\theta)t})\right] \tag{8}$$

where $p=p(t)$ in Eq. (8) is given by Eq. (7). Using some calculus, one finds as expected that $F(t)$, as given by the right-most expression in Eq. (8), strictly increases when D or λ increases or when the clearance rate, θ, decreases.

Furthermore, as noted in Brookmeyer *et al.* (2005), Eq. (8) reduces to a more useful form when the dose of inhaled spores is set to equal the toxic dose, $TD(p)$, defined as the dose giving a probability of infection equal to p. Carrying this out by using Eq. (6) to determine that $\ln(1-\pi)=-D\lambda/(\lambda+\theta)$, then replacing π by p (as used in $TD(p)$), and then substituting in the right side of Eq. (8) leads to:

$$F(t,p)=1-(1-p)^{(1-\exp(-(\lambda+\theta)t))} \tag{9}$$

where p is the probability of disease. Finally, because $\lambda \ll \theta$, the probability that the exposed subject becomes infected and that at least one spore germinates between time 0 and time t is approximated by

$$F(t,p)\approx 1-(1-p)^{(1-\exp(-\theta t))} \tag{10a}$$

The conditional probability $F^*(t,p)$ that germination of at least one spore takes place between times 0 and t given that infection does occur is $F(t,p)/p$, since here we are assuming the dose D gives a probability of infection equal to p, so

$$F^*(t,p)\approx\frac{1-(1-p)^{(1-\exp(-\theta t))}}{p} \tag{10b}$$

In the current work, the median time from exposure to germination following exposure to low doses of spores was predicted using Eq. (10b). As noted in Brookmeyer *et al.* (2005), as p approaches 0, F^* in Eq. (10b) becomes the cumulative distribution function (cdf) $1-\exp(-\theta t)$ corresponding to the exponential pdf $\theta\exp(-\theta t)$ whose median occurs at $t=\ln(2)/\theta$. The predictions were then compared with time-to-germination data collected in the rabbit following exposure to low doses of Ames spores. Because the inhaled doses were so low, we were not able to measure germination using standard dilution plate analysis (with and without heat kill) of homogenized tissue aliquots, so a quantitative PCR assay was developed (discussed below, Section 2.2.2).

2.1.4. Modified competing risks (MCR) model: bacterial replication, threshold and overall disease incubation period

Wilkening (2008) suggested the disease incubation period could be modeled using Sartwell (1950) classic log normal distribution. The general form of Sartwell's cumulative incubation distribution is:

$$F(t)=\left(\frac{1}{\sigma\sqrt{2\pi}}\right)\int_0^t\frac{1}{x}\exp\left(-\frac{(\ln x-\ln M)^2}{2\sigma^2}\right)dx \tag{11}$$

where M is the median incubation period and σ is the standard deviation of $F(t)$ when plotted against ln (t). Furthermore, Wilkening (2008) defined the incubation period as the time from germination to the point at which some threshold level of bacteria capable of inducing clinical disease (i.e., fever) is reached. In doing so, the following distribution was derived by Wilkening for the incubation period where the delay time from germination to symptoms, s, is treated as a random variable that follows a log normal distribution, $g(s)$, as follows

$$g(s)=\left(\frac{1}{\sigma_g\sqrt{2\pi}}\right)\left(\frac{1}{s}\right)\exp\left(\frac{(\ln(s)-\ln(T))^2}{2\sigma_g^2}\right) \tag{12}$$

In Eq. (12), T characterized the median time for bacterial growth and depended upon the empirically determined parameters in the following way:

$$T=\left(\frac{t_2}{24\ \ln(2)}\right)\bullet In\left(-\frac{24\ \ln(2)\ N_{\text{threshold}}}{\lambda t_2 D}\right) \tag{13}$$

where t_2 is the bacterial doubling time in hours, $N_{\text{threshold}}$ is the number of bacteria in the host tissue at the onset of symptoms, λ is the germination rate per day, and D is the dose. Thus, with the MCR model, the cumulative incubation period is the convolution of Eqs. (10b) and (12). The integral was numerically investigated by Wilkening (2008) but in the current work we approximated the solution by deriving the leading order term (see Supplemental Material for details). In doing so, the incubation period distribution was

$$F_{W,\,0}(t;\ \Lambda_W)=\frac{1}{2}(erf(\tau(t))+1)(1-e^{-(\theta+\lambda)t}) \tag{14a}$$

Where *erf* is the standard error function, the function $\tau(t)$ is defined as

$$\tau(t)\equiv\frac{\ln t-\ln T}{\sqrt{2}\sigma_g}$$

and the MCR density follows directly from Eq. (14a) via

differentiation and is

$$f_{W,0}(t;\ \Lambda_W) = \frac{1}{2}(\theta+\lambda)(erf(\tau(t))+1)e^{-(\theta+\lambda)t} + \frac{(1-e^{-(\theta+\lambda)t})e^{-\tau(t)^2}}{\sigma\sqrt{2\pi t}} \quad (14b)$$

2.1.5. Software

Unless otherwise noted, all calculations and figure plots related to the CR and MCR models were done using Mathematica 8. The PCR data shown in Fig. 2 was made using Statistica (StatSoft, Tulsa, OK).

2.2. Rabbit data collection

2.2.1. Rabbit exposures

2.2.1.1. B. anthracis Ames strain. A working stock (1 passage) of Ames strain bacteria (pXO1+ and pXO2+) was prepared from a seed stock. Spores were grown in trypticase soy broth supplemented with 100 mg/L manganese sulfate in a shaker incubator (225 revolutions per minute) at 37 °C for approximately 96 h. Spores were washed one time by centrifugation, resuspended in sterile phosphate buffered saline (PBS), and stored at 4–6 °C. Spores were heat shocked at 65 °C ± 2 °C immediately prior to use and the titer was determined before each exposure using standard dilution plating techniques. Resultant spore suspensions contained > 96% phase-bright spores.

2.2.1.2. New Zealand White (NZW) rabbits. Certified *Pasteurella*-free male NZW rabbits were obtained from Covance Research Products (Denver, CO) and weighed between 2–4 kg at the time of aerosol exposures. Rabbits were fed Teklad Certified Global High Fiber Rabbit Diet (Harlan Teklad, Madison, WI), 150 g, once daily and had unrestricted access to municipal water ad libitum. Controlled environmental conditions included temperature (18–29 °C), relative humidity (30–70%) and light (12 h on and 12 h off). In conducting this research, investigators adhered to the Guide for the Care and Use of Laboratory Animals (NIH publication 86-23, revised 1985).

2.2.1.3. Anthrax Vaccine Adsorbed (AVA) vaccination. Our primary interest was to assess low-dose–response in naïve hosts. However, some rabbits in the current work were vaccinated prior to exposure using a protocol known to provide complete protection (Pitt *et al.*, 2001). There were two reasons for vaccination in the current work. First, in the original competing risks model for inhalational anthrax, Brookmeyer *et al.* (2003, 2005) estimated lung spore clearance rate using historical NHP data originally published by Henderson *et al.* (1956). In those NHP studies, most of the monkeys were vaccinated prior to aerosol exposure. Thus, in order to provide a more meaningful comparison between the rabbit and NHP models, a portion of the rabbits in the current work were vaccinated prior to exposure. Second, and more importantly, vaccinated rabbits served as important controls that allowed us to better interpret data collected from naïve rabbits. As one example, Table 7 shows a large increase in vegetative bacteria in non-vaccinated (sham-vaccinated) rabbits beginning 24 h following exposure and a similar increase was not observed in fully protected vaccinated rabbits where the vaccination presumably prevented outgrowth. Furthermore, since rabbits were equally-dosed and exposed in pairs, one non-vaccinated rabbit paired with one vaccinated rabbit, and since all tissues were collected and processed side-by-side, it is unlikely that the increase in vegetative bacteria in only non-vaccinated rabbits 24 h following exposure was the result of germination and growth *ex vivo* during tissue processing.

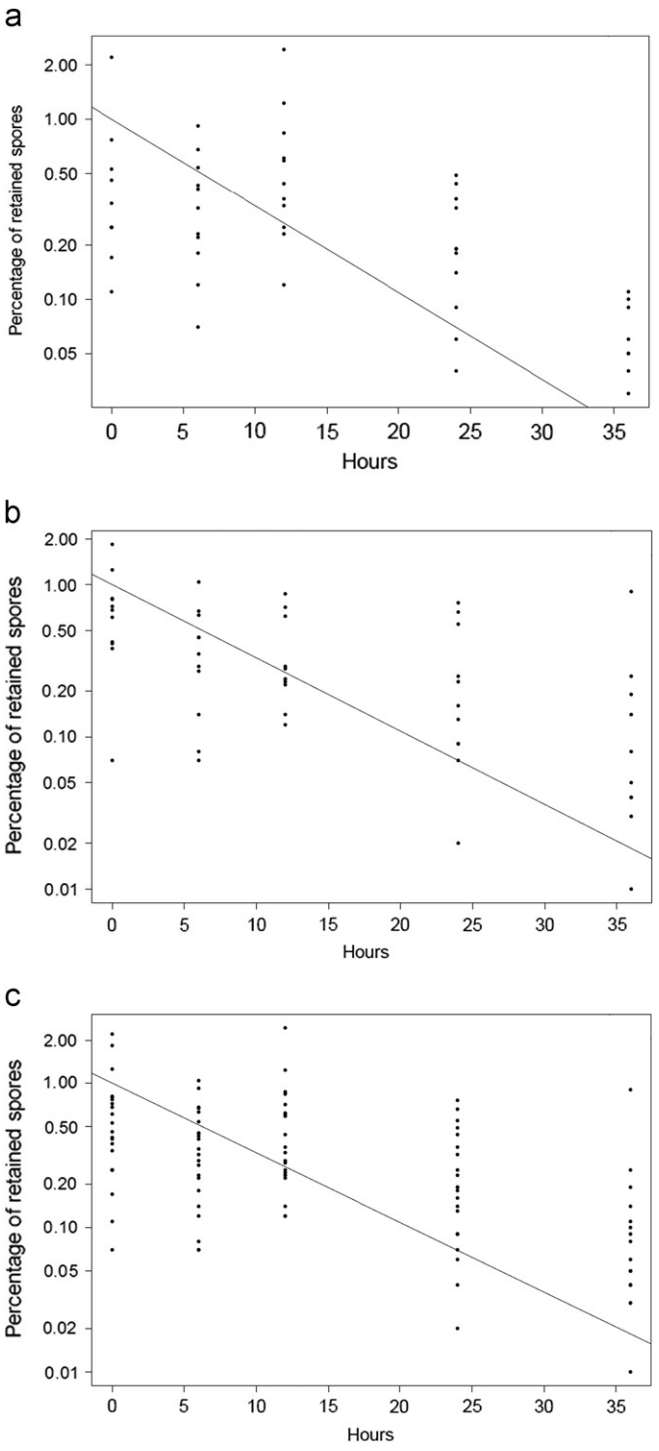

Fig. 1. The percent of retained (deposited) Ames spores remaining in rabbit lungs over time: individual animal data (dots) and fit (line). Groups of rabbits were exposed to known doses of Ames spores and at 0, 6, 12, 24 and 36 h post-exposure the numbers of spores in the lungs were determined in (A) sham-vaccinated, (B) AVA-vaccinated, and (C) pooled sham- and AVA-vaccinated rabbits. The data were then fit to an exponential decay model to determine clearance rate. The clearance rate was estimated at 4.69%, 4.77%, and 4.75% per hour in (A), (B), and (C), respectively.

Rabbits were vaccinated with an intramuscular injection of 0.5 ml Anthrax Vaccine Adsorbed (AVA) (BiothraxTM, Bioport Corporation, Lansing, MI; lot numbers FAV158, FAV114, FAV102 and obtained through MILVAX) or were sham-vaccinated with an

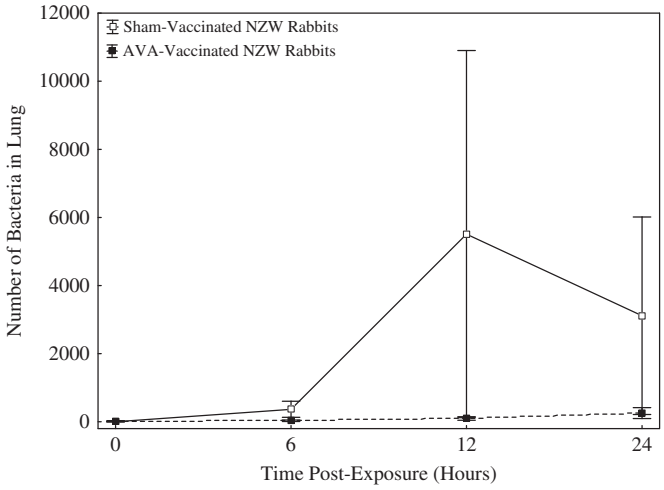

Fig. 2. Number of bacteria in the lung tissue following low dose exposure. Bacterial genomic target (BA-5435) copy numbers were determined by quantitative PCR from homogenized lung tissue in AVA-vaccinated (■) and sham-vaccinated (□) rabbits immediately following exposure (≈1 h) and at 6, 12 and 24 h post-exposure. The inhaled doses were 1493 ± 311 and 1424 ± 296 viable Ames spores for sham-vaccinated and AVA-vaccinated rabbits, respectively. All data are mean ± SEM with 6 animals per group except for hour 6, sham-vaccinated where there were 5 rabbits.

Table 1
Ames spore deposition in NZW rabbits.

Group	Delivered Dose (mean ± SEM) × 10^6	CFU Determined in Lung Homogenates (mean ± SEM) × 10^6	Percent deposited	Percent deposited (pooled)
Sham-vaccinated	16.39 ± 4.07	0.79 ± 0.39	4.33 ± 2.17	4.63 ± 1.10[a]
AVA-vaccinated	22.76 ± 2.71	1.10 ± 0.16	4.93 ± 0.81*	

* There was no significant difference between sham-vaccinated ($n=5$ rabbits) and AVA-vaccinated ($n=5$ rabbits) ($P=0.80$, Student's t test).

[a] In a independent study conducted under identical conditions, the percent deposition using 6 sham-vaccinated and 5 AVA-vaccinated rabbits was estimated at 4.39 ± 1.26% ($n=11$).

Table 2
Ames spore germination rate in NZW rabbits.

Dose	Germination rate	
	Spores per hour	Spores per day
Inhaled spores	3.14×10^{-7}	7.52×10^{-6}
Deposited spores	6.77×10^{-6}	1.63×10^{-4}

equal volume of PBS/2% Alhydrogel (Sham) (based on Pitt *et al.*, 2001). Alhydrogel was obtained from Brenntag Biosector (Frederikssund, Denmark). Injections occurred at week 0 (Day 0) and again at week 4 (Day 28) and the animals were challenged with aerosols of Ames spores at week 10 (day 70).

2.2.1.4. Bioaerosol challenge with B. anthracis Ames strain. Rabbits were weighed and randomly assigned to exposure groups and subgroups using a computerized data acquisition system (Path-Tox 4.2.2; Xybion, Cedar Knolls, NJ). Body weights of individual animals did not exceed ± 20% of the group mean. Rabbits were placed into muzzle-only exposure boxes for 10, 30, and 45 min on three consecutive days prior to bioaerosol challenge for conditioning. Unless otherwise noted, all exposures lasted 16 min which was the exposure time required to reach the targeted presented dose given experimental setup. Rabbits sacrificed at 6, 12, 24 or 36 h post-exposure were exposed in pairs—one AVA-vaccinated paired with one sham-vaccinated rabbit. Rabbits sacrificed immediately following the end of the exposure were exposed one at a time by alternating between one sham-vaccinated and one AVA-vaccinated animal. Spores were aerosolized in PBS plus 0.01% Triton-X using a 3-jet collison nebulizer. The mean mass aerodynamic diameter of the spores was 1.0 ± 0.3 μm as measured using a TSI Aerosol Particle Sizer (TSI, Inc., Shoreview, MN). Aerosols were collected in all glass impingers (AGI) containing PBS+0.01% Triton-X+antifoam. Aerosol dose (presented dose) was measured using a Buxco plethysmography system (Buxco Electronics, Wilmington, NC) on each animal. Animals were observed daily and moribund animals were euthanized immediately.

2.2.1.5. Effect of ex vivo tissue processing. There was concern that *ex vivo* tissue processing could alter the number and state of bacteria in the tissue and thus introduce artifacts into the data. As examples, tissue processing could cause dormant spores to germinate or processing could allow time for vegetative bacteria to replicate. We have previously shown that aerosolization renders a fraction of the spores heat sensitive (Gutting *et al.*, 2012), which is most likely due to damaged spore coats induced by the shearing forces placed on them during aerosolization. Here, examination of the spores recovered in the AGIs during exposure demonstrated 30.70 ± 2.7% ($n=60$ AGI/rabbit exposures) of the aerosolized spores were heat sensitive (Gutting *et al.*, 2012). It is noted that the spores were heat shocked prior to aerosolization according to standard methods. Thus, in our work, 30.7% of the inhaled spores were heat sensitive. Other investigators have made similar observations in the Ames spore/NZW rabbit model of inhalational anthrax [data collected from Battelle, page 22 of reference EPA (2011)]. To test the effect of our *ex vivo* tissue processing in the current work, a group of the rabbits were immediately sacrificed following exposure. The lungs were then immediately homogenized and the number of heat resistant and heat sensitive CFU were determined. The data showed that 30.5 ± 10.5% ($n=11$ rabbits) of the CFU recovered from the lungs were heat sensitive, which suggested our post tissue processing had no observable effect on the ratio of heat-sensitive to heat-resistance bacteria—that is, the spores were not germinating during tissue processing as measured by loss of heat resistance. We added peptone to our tissue homogenization buffer because we hypothesized that the peptone would help stabilize spores, particularly spores damaged from heat shock prior to aerosolization (Johnson and Busta, 1984). Although peptone contains amino acids, and high concentrations of certain amino acids are known to induce germination under the right conditions, ice-cold peptone was used herein to help stabilize spores. It is also noted that some investigators working with Sterne spores add peptone to their sporulation media (Pinzon-Areango *et al.*, 2010). The hypothesis that ice-cold peptone added to our tissue homogenization buffer would help stabilize spores and would not induce germination during the short time period required to process the tissue is supported by our data (mentioned above) and adds validity to the spore clearance data presented in Fig. 1. Furthermore, these observations also suggest that changes to the number of heat sensitive and heat resistant bacteria at later euthanasia time points (6–36 h) are the result of host–pathogen interactions prior to sacrifice, and are not due to artifacts introduced during tissue processing. Additional discussion is

Table 3
Low-dose attack rates calculated using the competing risks (CR) model and the fitted exponential dose-response (EDR) model for selected doses of inhaled Ames spores.

Dose (inhaled spores)[a]	Attack Rate (probability of disease for the given dose)	
	Competing risks (CR)[b]	Fitted exponential dose–response (EDR)[c]
98	0.000647	0.000708
286	0.00189	0.00206
767	0.00505	0.00552
2061	0.0135	0.0148
2678	0.0175	0.0192
13400	0.0847	0.0922
25388	0.155	0.168
105000	0.500	0.532

[a] The doses shown in this Table come from known dose-response data that have been collected in the lab for the NZW rabbit-Ames spore aerosol model (see Table 4 for publication/lab identification and responses).
[b] Attack rate derived using the CR model (Eq. (6)) where attack rate $=1-\exp^{-(\lambda/(\lambda+\theta))\mathrm{d}}$ with $\lambda/(\lambda+\theta)=6.605\times10^{-6}$
[c] Attack rate derived using the EDR model where attack rate $=1-\exp^{(-kd)}$ with $k=7.223\times10^{-6}$

Table 4
Comparison of laboratory dose–response data and the competing risks model dose response predictions for inhalational anthrax in NZW rabbits following inhalation of Ames spores.

Lab data: NZW rabbits/Ames spore aerosol					**Competing risks model predictions**										
Mean dose of inhaled spores	**# of Rabbits**	**Lab[a]**	**Observed survivors**	**Observed deaths**	**Probability of *n* number of deaths**										
					***n*=0**	***n*=1**	***n*=2**	***n*=3**	***n*=4**	***n*=5**	***n*=6**	***n*=7**	***n*=8**	***n*=9**	***n*=10**
98	10	1	10	0	0.994	0.006	$<10^{-4}$	$<10^{-7}$	$<10^{-7}$	$<10^{-7}$	$<10^{-7}$	$<10^{-7}$	$<10^{-7}$	$<10^{-7}$	$<10^{-7}$
286	5	2	5	0	0.991	0.009	$<10^{-4}$	$<10^{-7}$	$<10^{-7}$	$<10^{-7}$					
767	10	1	10	0	0.951	0.048	0.001	$<10^{-4}$	$<10^{-6}$	$<10^{-7}$	$<10^{-7}$	$<10^{-7}$	$<10^{-7}$	$<10^{-7}$	$<10^{-7}$
2061	5	2	5	0	0.934	0.064	0.002	$<10^{-4}$	$<10^{-6}$	$<10^{-7}$					
2678	4	3	4	0	0.932	0.066	0.002	$<10^{-4}$	$<10^{-7}$						
13,400	10	1	10	0	0.413	0.382	0.159	0.039	0.006	0.001	$<10^{-4}$	$<10^{-5}$	$<10^{-7}$	$<10^{-7}$	$<10^{-7}$
25,388	5	2	3	2	0.433	0.395	0.144	0.026	0.002	$<10^{-4}$					
105,000	10	1	5	5	0.001	0.010	0.044	0.117	0.205	0.246	0.205	0.117	0.044	0.010	0.001
275,094	5	2	1	4	$<10^{-3}$	0.003	0.030	0.155	0.400	0.412					
713,000	10	1	0	10	$<10^{-7}$	$<10^{-7}$	$<10^{-7}$	$<10^{-7}$	$<10^{-7}$	$<10^{-7}$	$<10^{-5}$	$<10^{-4}$	0.003	0.082	0.914
8,270,142	5	2	0	5	0	0	0	0	0	1					

[a] Lab 1Data were collected in 1995 at USAMRIID and were graciously provided courtesy of USAMRIID investigators. To our knowledge the specifics of the data set presented in this table have not been previously published, but these data have been summarized and/or cited by others (Coleman *et al.*, 2008; Zaucha *et al.*, 1998).Lab 2Data from EPA (2011).Lab 3Data was collected as part of the current research effort.

provided below with respect to tissue processing on PCR data, as well as bacterial replication data.

2.2.1.6. Deposited dose (lung tissue dose). Immediately following exposure, a selected set of rabbits was sacrificed and the deposited dose (lung tissue dose, retained dose) was determined as follows. Portions of the right middle lobe were removed, weighed (0.440 ± 0.001 g, average weight), and then homogenized in sterile PBS with 1% peptone at 4 °C using a tissue homogenizer (Precision disposable tissue grinder system, VWR Scientific). Then, a non-heated aliquot of the lung homogenate was plated on Tryptic Soy Agar (TSA) plates (Hardy Diagnostics, Santa Maria, CA), incubated overnight (37 °C), and enumerated using standard techniques. The resulting colony forming unit/ml (CFU/ml) data was converted to CFU/gram of recovered lung tissue using lung density (0.999 g/ml). Finally, all CFU/gram data was converted to total CFU per whole lung by using average lung weight data. Here, the average lung weight of five non-treated, age- and weight-matched control animals was determined to be 17.00 ± 2.4 g.

2.2.1.7. Spore clearance rate. At specified time points following exposure, rabbits were sacrificed and the numbers of spores (heat-resistant CFU; 65 °C ± 2 °C, 30 min heat kill) in lung tissue were enumerated using the dilution plate methods described above. Using this data, the fraction of spores remaining in a rabbit was calculated as the number of spores in the lung at a specified time point for a given animal divided by the number of spores that were deposited for that animal during exposure (deposited dose equaled the inhaled dose times 0.0463, see Table 1). Then, according to Brookmeyer *et al.* (2005), the spore clearance rate was derived by fitting an exponential decay model [$R=\exp(-\theta\ t)$, where R is the fraction of retained spores] by regressing $\log R$ on t. As with (Brookmeyer *et al.*, 2005), we did not include an intercept term because $R=1$ at time 0.

2.2.1.8. Germination rate. The germination rate was determined by following the method used by Brookmeyer *et al.* (2005). The inhaled dose found to induce an attack rate of 0.50 (i.e., LD_{50}) in NZW rabbits is pubished at 1.05×10^5 fully virulent Ames spores (Zaucha *et al.*, 1998). Using this data and the clearance rate (derived in the current work), one can rearrange Eq. (6) to acquire the germination rate; $\lambda=\theta\ \ln(2)/(LD_{50}-\ln(2))$.

2.2.2. Bacterial enumeration using PCR

Immediately following animal sacrifice, the right middle lobe was excised, weighed, homogenized in sterile PBS with 1%

Table 5
Comparison of laboratory dose–response data and the competing risks model dose–response predictions for inhalational anthrax in NZW rabbits following inhalation of Ames spores using varying LD_{50} values.

AdjustedLD_{50}	Mean dose of inhaled spores	Competing risks model predictions Probability of n number of deaths									
		$n=0$	$n=1$	$n=2$	$n=3$	$n=4$	$n=5$	$n=6$	$n=7$	$n=8$	$n=9$	$n=10$
85,000	2678	0.916	0.081	0.003	$<10^{-4}$	$<10^{-6}$						
	13,400	0.335	0.387	0.201	0.062	0.125	0.002	$<10^{-3}$	$<10^{-4}$	$<10^{-6}$	$<10^{-7}$	$<10^{-7}$
	25,388	0.355	0.408	0.188	0.043	0.005	$<10^{-3}$					
95,000	2678	0.925	0.073	0.002	$<10^{-4}$	$<10^{-6}$						
	13,400	0.376	0.386	0.179	0.049	0.009	0.001	$<10^{-4}$	$<10^{-5}$	$<10^{-6}$	$<10^{-8}$	$<10^{-10}$
	25,388	0.396	0.403	0.164	0.033	0.003	$<10^{-3}$					
115,000	2678	0.937	0.061	0.001	$<10^{-4}$	$<10^{-7}$						
	13,400	0.446	0.375	0.142	0.032	0.005	$<10^{-3}$	$<10^{-4}$	$<10^{-5}$	$<10^{-7}$	$<10^{-9}$	$<10^{-11}$
	25,388	0.465	0.385	0.127	0.021	0.002	$<10^{-4}$					
125,000	2678	0.942	0.056	0.001	$<10^{-4}$	$<10^{-7}$						
	13,400	0.476	0.367	0.127	0.026	0.004	$<10^{-3}$	$<10^{-4}$	$<10^{-6}$	$<10^{-7}$	$<10^{-9}$	$<10^{-11}$
	25,388	0.494	0.374	0.113	0.017	0.001	$<10^{-4}$					

Table 6
Median Germination Periods, as a Function of Toxic Dose, in NZW Rabbits Following Aerosol Exposure to Ames Strain *B. anthracis*.

Dose [*TD*(*P*)][a]	Median time to germination (h)
TD(1)	14.54
TD(10)	14.05
TD(25)	13.14
TD(50)	11.29
TD(95)	5.10
TD(99)	3.38

[a] *TD*(*P*) is the dose estimated to induce *P*% disease in NZW rabbits. For example, *TD*(95) is a high dose of spores estimated to induce disease in 95% of exposed rabbits.

Table 7
Number of heat resistant and heat sensitive CFU in sham-vaccinated and AVA-Vaccinated rabbit lungs 6–36 h post-exposure.

Time post-exposure (h)	Heat resistant CFU/lung ($\times 10^5$)	Heat sensitive CFU/lung ($\times 10^5$)
Sham-Vaccinated		
6	4.96 ± 1.05	1.40 ± 0.67
12	6.74 ± 2.84	1.05 ± 0.85
18	ND	ND
24	2.40 ± 0.50	11.58 ± 7.33
30	ND	ND
36	2.95 ± 0.71	35.51 ± 2.12
AVA-Vaccinated		
6	5.16 ± 0.15	2.49 ± 0.99
12	2.98 ± 0.15	3.08 ± 1.68
18	ND	ND
24	3.69 ± 1.27	3.74 ± 1.18
30	ND	ND
36	1.57 ± 0.45	1.49 ± 0.58

peptone at 4 °C using a tissue homogenizer (Precision disposable tissue grinder system, VWR Scientific), frozen and stored at −80 °C until DNA was extracted. At that time, frozen lung homogenates were thawed and 1 ml aliquots were removed from each sample. Pellets were formed by centrifugation of the aliquots by centrifuging at 6000*g* for 5 min, and supernatants were removed. Each pellet was weighed in pre-weighed tubes to determine pellet weight. All pellets were resuspended in 200 μl sterile PBS. DNA was isolated from the pellet by bead-mill homogenization in 180 μl ATL (tissue lysis buffer, Qiagen, Valencia, CA), 20 μl Proteinase K and 20 μl Antifoam B, using a FastPrep bead-mill homogenizer (MPBio, Solon, OH) for 40 s at 6.0 m/s (MPBio, Solon, OH) using lysing matrix B tubes. Samples were incubated at 56 °C for 30 min and were subsequently amended with 4 μl RNase A (100 mg/ml), mix and allowed to incubate at room temperature for 2 min. 200 μl Lysis buffer AL (Qiagen, Valencia, CA) was added and each sample was allowed to incubate at 70°C for 30 min. Homogenates were centrifuged at 13,000*g* for 5 min, and supernatants containing DNA were removed (~400 μl/sample). 200 μl 100% ethanol was added and mixed with homogenates and entire volume was added to the QIAamp DNA spin columns (Qiagen, Valencia, CA). Spin columns were centrifuged for 1 min @ 6000*g* and flowthrough was discarded. Columns were then washed with AW1 and AW2 (500 μl each) with centrifugation steps included (6000*g* for 1 min in between washes, and 13,000*g* for 3 min to dry column). Final elution was performed by adding 200 μl of pre-warmed Buffer AE, allowing solution to incubate at room temperature for 1 min, and centrifuging for 1 minute at 6000*g*. Original volume of AE was replaced on column and centrifuged once more to increase yield of recovered DNA.

The nucleotide sequences of *B. anthracis* Ames chromosomal target BA_5345 (NC_003997) were obtained from the National Center for Biotechnology Information (NCBI). Primer express v3.0

(Applied Biosystems, Foster City, CA) was used to design upstream and downstream primers for cloning using published sequences for BA_5345 (Antwerpen *et al.*, 2008). *B. anthracis* PCR products used for cloning segments of BA_5345 were produced with a PCR thermal cycler profile of 95 °C for 5 min, 40 cycles of 95 °C for 30 s, 56 °C for 1 min, 70 °C for 1 min with a final extension at 70 °C for 8 min. A portion of the PCR product (20 μl) was separated on 1.25% agarose gels to confirm the size and singularity of the amplicons and were then ligated to the pCRII TOPO vector (Invitrogen, Carlsbad, CA). Plasmids were used to transform TOP 10 *E. coli* chemically competent cells. Plasmid DNA was isolated from late-log phase cultures using Qiagen Miniprep Plasmid DNA kits (Qiagen, Valencia, CA). Gene-specific Primers and M13 (-20) reverse or forward primers were used to determine orientation of the clone by sizing of amplicons using gel electrophoresis. Clones identified as containing the correct size and orientation of the insert were selected and grown in larger volumes of LB overnight at 37 °C and plasmid DNA was isolated using the Qiagen Midiprep Plasmid DNA kit. Plasmid DNA was linearized using EcoRV (Promega, Madison, WI) and purified using QIAquick spin columns.

To quantify bacterial numbers following low-dose exposures, absolute quantification of BA_5345 was performed using the ABI7500 Absolute Quantification method. Briefly, standard curves are generated by amplifying known amounts of linearized standards. Optical densities for the standard samples were measured spectrophotometrically, and copy numbers were calculated using the known size of the linearized plasmid. Dilutions of the linearized plasmid standards (1:10 serially) and 10 μl of sample DNA were added to PCR mastermix containing 1 μM forward/reverse primer and 0.8 μM probe concentrations and plated in optical plate wells. Amplification was carried out using a thermal cycle profile of 95 °C initial denaturing step, and 40 cycles of 95 °C for 15 s, 60 °C for 1 min for primer annealing and product extension. Cycle thresholds and baseline measurements were determined automatically by the Applied Biosystems SDS v1.3.1 software and were compared with previous and subsequent runs for similar DNA samples. Absolute quantification profiles were calculated for each unknown DNA sample on the plate by comparison to the standard curve values using the SDS v1.3.1 software. Individual pellet weights from which the DNA was originally extracted and the average weight of the entire rabbit lung was used to calculate total chromosomal targets in the lung from the absolute quantification profile.

3. Results

3.1. Spore deposition (lung tissue dose)

The first step in estimating the rate of Ames spore clearance from the lung, θ, was to estimate the number of spores deposited during aerosol exposure (i.e., deposition/lung tissue dose). Here, groups of vaccinated (see Section 2.2.1 for justification on why vaccinated rabbits were used) and non-vaccinated rabbits were exposed to high doses (>100 LD_{50}) of aerosolized Ames spores and immediately following the exposure, portions of the lungs were removed, homogenized, and plated to quantify bacteria. As shown in Table 1, $4.33 \pm 2.2\%$ of the inhaled dose was recovered in lung homogenate of sham-vaccinated rabbits ($n=5$), and $4.93 \pm 0.8\%$ from AVA-vaccinated rabbits ($n=5$). Because there was no significant difference between sham-vaccinated and AVA-vaccination rabbits ($P=0.80$, Student's t test), these data were pooled ($n=10$) and results suggested 4.63% of the inhaled spore dose was retained/deposited in the lungs during exposure. In an independent study that used 11 rabbits (6 sham-vaccinated and 5 AVA-vaccinated), 4.39% of the inhaled dose was recovered in lung homogenate immediately following exposure (data not shown).

3.2. Ames spore clearance rate and germination rate

To determine spore clearance rate, the fraction of spores remaining in the lung over time was determined. Here, groups of rabbits were exposed and the deposited dose was calculated using deposition data presented in Table 1 (4.63% of inhaled dose). Then, at specified time points post-exposure (up to 36 h), a portion of the rabbits were sacrificed and the number of spores in the lung was determined. Data collection stopped at 36 h because by this time several of the non-vaccinated rabbits were bacteremic and had succumbed to the systemic infection. Fig. 1 shows the fraction of spores remaining in the lung over time where each data point/dot in the graph represents a single rabbit. The data presented were pooled from two separate studies conducted 14 months apart. These data show a steady decrease in the number of spores over time in both sham-vaccinated (Fig. 1A) and AVA-vaccinated rabbits (Fig. 1B). The clearance rate, θ, was 4.69% and 4.77% per hour in sham-vaccinated and AVA-vaccinated rabbits, respectively. Because there was no significant difference between sham-vaccinated and AVA-vaccinated rabbits, all the data were pooled and the clearance rate of Ames spores from NZW rabbit lungs was determined at 4.75% per hour (Fig. 1C).

Following Brookmeyer *et al.* (2005), Eq. (6) was then used to derive the germination rate. Here, the clearance rate equaled 0.0475 spores per hour and the LD_{50} was 1.05×10^5 (Zaucha *et al.*, 1998). As shown in Table 2, the germination rate was estimated at 3.14×10^{-7} inhaled spores per hour or 7.52×10^{-6} inhaled spores per day. When derived as a function of deposited dose, the germination rate was estimated at 6.77×10^{-6} spores per hour (1.63×10^{-4} per day).

3.3. Low dose extrapolation using the CR model

The next aim was to use Eq. (6) to extrapolate to low doses and then compare the model attack rate with known low-dose laboratory data as well as the attack rate when the entire dose response curve was fit to the EDR model.

To our knowledge, there are only three data sets available where groups (>3 animals) of NZW rabbits have been exposed to low (non-lethal) aerosol doses of Ames spores. These data sets are presented in Tables 3–5 along with model predictions. The three data sets have been collated by dose, starting with the lowest. One of the data sets was provided courtesy of USAMRIID investigators [Lab 1] where five groups of rabbits (10 rabbits per group) were exposed to varying doses of Ames spore aerosols. The dose ranged from a mean of 98 inhaled spores for the low dose group up to 713,000 spores in the highest dosed group. As shown in Table 4, all 10 rabbits exposed at the high dose succumbed to the infection, half of the 105,000 dose group succumbed (this dose group/data is often cited as the rabbit LD_{50} (Coleman *et al.*, 2008; Zaucha *et al.*, 1998)) and there were no observed deaths for the three lowest dosed groups. The second data set [Lab 2] was from a study conducted by EPA (EPA 2011). Here, groups ($n=5$ rabbits per group) were exposed to Ames spore aerosols ranging from a mean spore dose of 286 spores up to greater than 8 million spores. As shown in Tables 4, 2/5 and 4/5 rabbits in the 25,388 and 275,094 spore dose groups, respectively, succumbed to the infection. Finally, as part of the current research effort, a single group of 4 rabbits were exposed to a mean aerosol dose of 2678 spores at the Lovelace Respiratory Research Institute [Lab 3] and there were no observed mortalities (Table 4).

The competing risks model low-dose–response predictions associated with these low exposure doses are shown in Table 3 and compared with the EDR predictions. As shown, the probability of disease following exposure to 98 spores was 6.47×10^{-4} and 7.08×10^{-4} for the CR and EDR models, respectively.

The attack rates just discussed are for a single rabbit. To provide more real world predictability for the laboratory investigator, we next calculated the number of deaths that could be expected given an inhaled dose and a specific rabbit population size. Based on binomial probability calculations, the results are shown in Table 4 and show good agreement with the experimental data. For example, if an investigator exposed 10 rabbits to a mean inhaled dose of 767 spores (third lowest dosed group in Table 4) there is a 95.1% probability that zero deaths ($n=0$) will be observed in that study, 0.9% chance that 1 death would be observed, and so on up to the probability that all 10 rabbits would die. This prediction agrees well with observations made in Lab 1, where 10 rabbits were exposed to this dose and zero deaths were observed. This type of information could be very useful in designing both low- and high-dose experiments where a given number of responders are required.

The LD_{50} value used in the current work (105,000 Ames spores) is published but the raw data and methods used to derive that number are not published. Thus, there is a higher degree of uncertainty in the LD_{50} value than there is for other data. For example, the clearance rate was derived in the current work from two independent studies and the dose–response data is data from three different labs. To begin to examine what affect variation and sensitivity the LD_{50} value has on model predictions, we examined the attack rate using different LD_{50} values ranging from 85,000 to 125,000. The results are shown in Table 5 for three low-dose groups chosen from the dynamic part of the low-dose–response curve (2678, 13,400 and 25,388) where lethality is first observed.

3.4. Low-dose germination period, CR model predictions and low-dose laboratory data

The competing risks model (Eq. (10b)) was used to predict the low-dose germination period as a function of toxic dose, p. A clearance rate of 4.75% spores per hour (Fig. 1C) was used. For low-doses, the median germination period in the limit as the probability of infection p goes to 0 is $\ln(2)/\theta = 14.59$ h. Table 6 shows predicted germination periods for defined doses using Eq. (10b). High-dose germination periods are shown, but it is noted that Eq. (10b) applies to low doses. As shown, a dose associated with 1% lethality was associated with median germination periods of 14.54 h.

To test this prediction, rabbits were exposed to low doses of Ames spores and at specified time points following exposure the lungs were removed and assessed for signs of Ames spore germination. The mean dose of inhaled spores was 1493 ± 311 and 1424 ± 296 viable Ames spores in sham-vaccinated and AVA-vaccinated rabbits, respectively. This suggested, based on percent deposition (see Table 1), approximately 70–80 viable Ames spores were deposited in the lungs. Such a low number of spores proved to be below the limit of detection using standard dilution plate assays from homogenized lung tissue (data not shown). We therefore opted to use quantitative PCR against an Ames-specific chromosomal marker, BA_5345, to assess germination. As shown in Fig. 2, bacteria were not detected in the lungs of any rabbit on study using PCR immediately following exposure, and bacteria were not detected in vaccinated rabbits at any time point examined following exposure. In contrast, Ames genes were detected in sham-vaccinated (naïve) rabbits 12 h following exposure (solid line, Fig. 2). Here, 2 of the 6 rabbits (33%) had detectable Ames genes (see Supplemental Data for *Ct* values). Because germination is tightly associated with DNA replication and in vivo DNA replication will increase the number of DNA targets in the tissue above the limits of detection (so it is now being detected in the tissue), the results suggested spores were germinating only in sham-vaccinated rabbits and only after approximately 12 h post-exposure- i.e., the observation is not made at 0 or 6 h post-exposure, a time point when there are more spores in the lungs and therefore the 12 h time point observations are not likely the result of *ex vivo* tissue processing. It is also noted that the tissue were kept on ice until the DNA was extracted, thus there would be little polymerase activity while the tissues were being homogenized. These low-dose time-to-germination data are in excellent agreement with the low-dose CR germination period predictions (Eq. 10a and b).

3.5. Incubation period: modified competing risks (MCR) model

The aim in this part of the work was to evaluate the low-dose incubation period distribution using the MCR model, using Eq. (14a and b) as described by Wilkening (Wilkening, 2008). A summary of the parameter values that were used is shown in Table 8. Clearance and germination rates were 0.475 per hour and 3.14×10^{-7} per hour, respectively. The dose of spores was set to 1 bacterium, regardless of the exposure dose, because disease incubation period begins with the first replicating bacteria (Wilkening, 2006), which is approximately 12–14 h following exposure for a low dose (discussed above: Table 6, Fig. 2). The bacterial doubling time, t_2, is the average time required for bacteria to double. In the current work, we derived t_2 using two different sets of data- both were data from the lung but one was collected following high dose exposure (CFU data) and the second was from low dose exposure (PCR data). In the first, the total number of vegetative bacteria in the lung was measured over time using standard dilution plate assays following a high dose exposure. As shown in Table 7, there was a rapid increase in the number of vegetative cells in the lung between 12 and 24 h post-exposure, which was concomitant with a decrease in the number of spores. These increases in heat sensitive CFU in the lungs of non-vaccinated rabbits, with no observable increase in AVA-vaccinated rabbits, is consistent with vaccine protection where bacterial growth is inhibited. Thus, using the data from naïve rabbits, the bacterial doubling time was estimated at 4.4066 h using the high dose data. Detection of heat-sensitive CFU early in the infection (6 h) is most likely due to damaged spores that have not been cleared and are not germinating spores, and the heat-sensitive CFU detected at 12 h are most likely a combination of ungerminated damaged spores and germinating spores. Regardless, the doubling time was determined from the 24 and 36 h time point data. The doubling time was also estimated using lung data from rabbits exposed to low-doses of spores. Here, rabbits inhaled < 2000 spores and the bacterial doubling time was estimated at 1.906 h (using data from Fig. 2). For comparison, the bacterial doubling time for man/monkey was estimated at 1.81 h (Wilkening 2008). For $N_{threshold}$, which is the threshold number of bacteria required to cause fever, we used a value of 1.0×10^6

Table 8
Parameter values log-normal disease incubation period.

Parameter	Value	Units
θ	0.0475	h^{-1}
λ	3.14×10^{-7}	h^{-1}
σ	0.53227	Unitless
t_2	4.4066	h
$N_{threshold}$	10^6	CFU
D	1	CFU

vegetative bacteria. This value is the number of bacteria 24 h post-exposure (Table 7) corresponding to the approximate mean time from exposure to pyrexia in the rabbit inhalation anthrax model (29–33 h; from (Yee *et al.*, 2010)). For σ_g, the standard deviation of the bacterial growth time distribution and was estimated at 0.532. Thus, the rabbit σ_g used in the current work agrees well with that estimated for the monkey—0.412 (Wilkening, 2008). Using these data, the incubation period distribution (Fig. 3) suggested the mean incubation period was 14.7 and 16.8 days based on low-dose PCR data and high-dose dilution plate doubling time data, respectively. For comparison, the MCR model estimated a low-dose incubation period for the Sverdlovsk victims of 9.04 days (Wilkening, 2008).

4. Discussion and conclusions

There is a need to improve our ability to conduct human risk assessments following inhalation of a low number of *B. anthracis* spores. Given the nature of the disease and the pathogen, it is essential to couple data collection and computational models while moving towards this goal. This approach will not only benefit risk assessors and risk managers, but will also provide useful tools to help guide the experimentalist. The work described in the current manuscript coupled data collection with the CR and MCR model of inhalational anthrax to further advance our understanding of low-dose inhalational anthrax in the rabbit.

The initial aim of this work was to derive the spore clearance rate and spore germination rate following high dose exposure, and then use these parameter values to generate a low dose-attack rate using Eq. (6). In order to derive spore clearance from the lung over time, it was necessary to first determine the number of spores deposited in the lung during aerosol exposure. The deposited/lung tissue dose was determined by quantifying bacteria using standard dilution plate analysis in homogenized lung tissue obtained immediately following exposure to high doses of spores. Data from two independent studies, 22 rabbits in total, suggested between 4.33% and 4.93% of the inhaled dose was deposited in the lung (Table 1). These data are based on recovery and dilution plate analysis of viable spores obtained from homogenized lung tissue. To our knowledge, there is no published deposition data available in the rabbit-Ames spore aerosol model to compare this data against. However, these deposition data are in good agreement with a preliminary spore deposition computational model developed for the rabbit (Gutting *et al.*, 2008). Here, rabbit lung morphometry was coupled with the physical factors known to dictate particle flow and retention in the airways (such as spore size and airway branching) and predicted between 4-5% of the inhaled spore dose would be deposited in the rabbit lung. In addition, these deposition values are not statistically different from data obtained when deposited spores were quantified using bronchoalveolar lavage (data not shown). It is also worth noting that spores were quantified in rabbit lungs using identical methods for all time points tested (0–36 h), and whatever error is associated with the deposited spore determination would most likely apply to all the data and uniformed scaling all the data will not affect the rate of clearance.

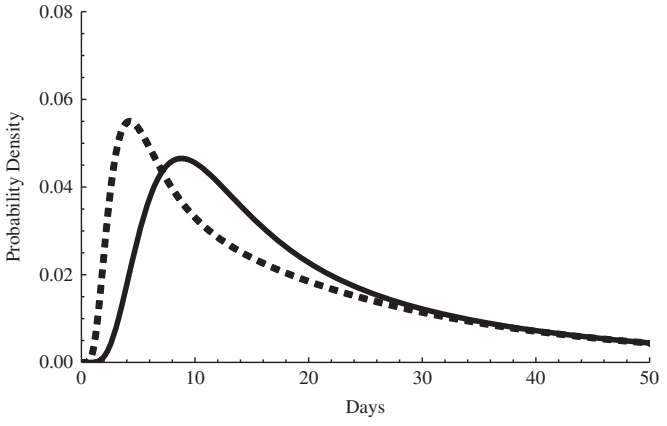

Fig. 3. Cumulative distribution and probability density function for low-dose incubation period in NZW rabbits following exposure to aerosols of Ames spores. For the dashed line, calculations were made using bacterial replication rate obtained from PCR data. For the solid line, calculations were made using bacterial replication rate obtained from dilution plate data.

With an estimate of the number of spores deposited in the lung during exposure, it was now possible to determine the fraction of spores remaining in the lung over time. Following the methods described by Brookmeyer *et al.* (2005), spore clearance data was fit to an exponential decay model which yielded a clearance rate of 4.75% per hour in the rabbit (Fig. 1). This is considerably faster than the 7% per day estimated by Brookmeyer *et al.* (2003, 2005), who based their rate on the historical monkey data published by Henderson *et al.* (1956). However, the faster clearance rate in rabbit is consistent with the observation that overall disease kinetics is faster in rabbits than other species such as monkeys (Zaucha *et al.*, 1998; Twenhafel, 2011). It should also be noted that in the work of Henderson *et al.* (1956), the monkeys survived up to 100 days following exposure because they were treated with a combination of antibiotics and vaccination, and the 7% per day clearance rate was derived from data collected between 40–100 days post-exposure. Because investigators have long hypothesized that antibiotics like penicillin can have a static affect on spores and cause them to persist in tissue (Barnes, 1947; Friedlander *et al.*, 1993), it is unclear if the clearance rate immediately following exposure in naïve monkeys is the same as that obtained under experimental conditions used with the historical monkey data study. The rate may, in fact, be more similar to the rabbit rate derived in the current work.

Spore germination rates are inherently difficult to measure in vivo for a number of reasons (Gutting *et al.*, 2012). As a result, it was not possible to directly measure the germination rate in rabbits in the current work. We therefore followed the approach used by Brookmeyer *et al.* (2005) and derived the germination rate using Eq. (6) coupled with the published rabbit LD_{50} data (1.05×10^5; (Zaucha *et al.*, 1998)) and the spore clearance rate. The germination rate in the rabbit was determined at 7.5×10^{-6} per day based on inhaled spore dose (Table 2). This is comparable to the germination rate (Brookmeyer *et al.*, 2005) for the monkey model which ranged between 5×10^{-7} and 1×10^{-5} inhaled spores per day, depending on which monkey LD_{50} value those authors used in the calculation.

It was now possible to use Eq. (6) to conduct a low-dose extrapolation and compare low-dose model predictions against known low-dose data, as well as against predictions made by fitting the entire dose–response curve to an exponential distribution- the EDR model. Based on guinea pig and NHP inhalational anthrax dose–response data, the EDR provided the best fit (Bartrand *et al.*, 2008; Haas, 2002; Huang and Haas, 2009). In the EDR model, the dose-response parameter, k, was determined at 7.22×10^{-6} for the rabbit data which predicted an attack rate of 7.22×10^{-5} for an inhaled dose of 10 spores. For the CR model, the attack rate using Eq. (6) for inhalation of 10 spores was 6.61×10^{-5}. Thus, disease probability in the low-dose exposure range predicted using the CR model and the EDR model are essentially the same. These results demonstrate that the actual rabbit low-dose response (lethality) curve can be accurately described using high-dose clearance and germination data (i.e., without any low dose data), and opens the door for the possibility of conducting

credible low dose extrapolations using only high dose data. And, perhaps more important, demonstrates an accurate low-dose extrapolation for a response based on mechanistic data (germination and clearance rates) rather than simply fitting actual response data. This suggests that human clearance and germination estimates obtained from in vitro, *ex vivo* or computational models could be used to develop a low-dose–response inhalational anthrax model in man (discussed further below).

There are several assumptions in the model. The first is that germination of a single spore is sufficient to cause lethality. This assumption is nearly impossible to prove in the lab although one dose-response study suggested lethality was observed in a marmoset following inhalation of 14 spores (Lever *et al.*, 2008). If deposition in marmosets can be approximated by the deposition data presented here for rabbits, then the animal died following deposition of just a few spores. Another assumption in the model is that germination and clearance are independent events. It has been proposed that germination may lead to increased spore killing and germination thereby indirectly contributes to spore clearance (Welkos *et al.*, 2001, 2002). How this potential relationship factors into the CR model remains to be determined. An additional assumption is that each spore germinates independently of each other. Given the role of quorum sensing in spore germination with *Bacillus* species (Zhang *et al.*, 2011; Fujiya *et al.*, 2007; Caipo *et al.*, 2002), it is possible that this assumption is not valid—at least following exposure to a high dose of spores where large clusters of spores would be deposited in a local area of the lung. However, following inhalation of a few hundred spores, and the resulting deposition of only tens of spores, it could be argued that the density of deposited spores would be too low to allow effective communication during the disease initiation phase of infection. A final assumption in the CR dose–response model, Eq. (6), is that spore clearance and germination rates are independent of dose. It is currently unknown if the rates presented in the current work are dose-dependent or constant throughout the entire dose range.

There are many reasons why understanding the disease incubation period is important for inhalational anthrax. Disease incubation information can be used to guide biomonitoring efforts, help determine the end of an anthrax outbreak, and through backtracking movements, it could be used to identify point release locations. While traditional risk assessments are largely concerned with predicting overall outcome of the exposure to a given dose, disease incubation period information can be used to support risk assessments in other key ways. As an example, how long do you hold and monitor research animals following low-dose exposure before you can conclude the animal will not develop inhalational anthrax? This is an important consideration given the significant costs associated with conducting aerosol exposures in high containment laboratories using select agents like Ames strain *B. anthracis,* as well as with simply holding larger animals like monkeys, guinea pigs and rabbits for lengthy periods of time in high containment labs. Understanding disease incubation in animal models would help reduce costs and eliminate false negative outcomes resulting from terminating studies prematurely.

Finally, disease incubation period models could help strengthen and validate dose–response models if there are parameters common to both models. The current work is an example of this concept. The incubation period predicted for low dose exposure using the MCR model was between 14.7 and 16.8 days, which is clearly a reasonable estimate for low dose disease incubation in the rabbit (EPA, 2011). This suggests the disease incubation period model parameter values are accurate and two of these parameters, germination and clearance rates, are used in the CR overall dose-response model.

Although the CR and MCR low-dose extrapolations presented in the current work (i.e., low-dose attack rate, low-dose germination period, and low-dose disease incubation period) are consistent with available low-dose rabbit data, there was concern that the data/parameters used could be skewed from artifacts introduced while the tissues were processed *ex vivo* and in particular, the potential for germination and growth while tissues were processed. There are three data sets in this paper where this type of error could be introduced: the high-dose spore clearance plate data (Fig. 1), the low-dose PCR-based doubling time data (Fig. 2), and the high-dose bacterial doubling time plate data (the 24 and 36 h naive rabbit data presented in Table 7). The data in Fig. 2 are PCR data for a bacterial chromosomal gene. The only use of this PCR data in the model was to estimate bacterial doubling time, t_2, for Eq. (13). Here, the lungs were immediately placed in ice-cold homogenization buffer and kept on ice until the DNA was extracted and since polymerases are essentially inactive at 4C, it is highly unlikely that the increases in PCR targets seen only at 12 and 24 h, and only observed in sham-vaccinated rabbits, are the result of *ex vivo* DNA replication of bacterial chromosome. Likewise, with respect to data presented in Table 7 (whose use was as a second estimate of bacterial doubling time, t_2), it is highly unlikely that the increases in CFU observed only at 24 and 36 h, and only in sham-vaccinated rabbits, are the result of *ex vivo* growth while the tissues were processed on ice because, again, growth requires active enzymes, like DNA polymerases, and for this reason bacteria essentially show no growth when kept cold for short periods of time. It is therefore reasonable to suggest that if there is error introduced into the model as a result of *ex vivo* tissue processing, that error will be associated with the data presented in Fig. 1 (spore clearance, i.e., quantification of heat-resistant CFU over time). Although the data presented suggested germination (loss of heat resistance in a plate assay) was not occurring while tissues were processed – 69.3% of the inhaled CFUs were heat-resistant and 69.5% of the CFUs recovered from processed lung tissue obtained immediately following exposure were heat-resistant – the potential for *ex vivo* germination was still a concern. To further address this, we developed and ran the CR and MCR models using total CFU clearance data rather than only using the heat-resistant CFU clearance data. Thus, in effect, we allowed for as high as 100% germination *ex vivo*, even though there are significant spores detectable in all lung samples at all time points. Here, we used the same lung CFU data that is shown in Fig. 1 except the 24 and 36 h naïve data were eliminated because at these time points there are clear signs of increased bacterial numbers in the lung due to bacteremia (see Table 7). When using total CFU rather than heat-sensitive CFU, lung clearance changed from 4.75% per day to 3.96% per day. The low-dose median time to germination changed from 14.54 h to 17.44 h. The median low-dose incubation period range changed from 14.7–16.8 days to 17.5–19.0 days. Considering these changes are introduced by assuming 100% *ex vivo* germination, the model does not appear sensitive to error introduced from a small undetectable percent of spores that could be germinating while the lung tissues were processed. The two primary reasons why the model is not sensitive to *ex vivo* germination error is because germination period, λ, is derived using Eq. (6); it is not directly measured in the current work. *Note*: although we claim the PCR data suggests a 14.5 h germination period, this data was never used in the model to defineλ. And second, physical clearance is the dominant process in the competing risks model such that germination period is eliminated from the model completely when examining disease incubation period ($\lambda \ll \theta$, see Eq. (10b)).

A thorough discussion on how to use the CR and MCR models to support cross-species extrapolation to man is well beyond the scope of the present paper, but there are several points worth noting. Foremost, if the models are to be used directly to develop a human low-dose response curve then the human parameter values would need to be determined. One approach to estimate

human parameter values would be to conduct side-by-side in vitro or *ex vivo* studies using human and animal materials/reagents. An example would be to compare and contrast macrophage–spore interactions using tissue culture methods (Gutting *et al.*, 2005) or comparing bacterial replication rates in species-specific media such as sera (Bensman *et al.*, 2012). If these in vitro/*ex vivo* animal data could be extrapolated to the animal in vivo model then in vitro/*ex vivo* human data could be used to parameterize a human in vivo computational low-dose–response and disease incubation period model. This is in effect using an animal model to validate animal tissue culture data and then using human tissue culture data to develop a human in vivo model. A second approach that could be used to estimate human parameter values would be through the use of additional computational models. For example, in addition to the CR and MCR models described herein, physiologically-based biokinetic (PBBK) models and deterministic models of inhalational anthrax are being developed (Gutting *et al.*, 2008; Day *et al.*, 2011; Kumar *et al.*, 2008). While we typically think of these models being used to predict overall disease outcome (i.e., the response), they could be modified such that they predict parameter values, or at least help to validate parameter values. A PBBK-like model that predicts spore clearance rate, rather than a PBBK-like model that used spore clearance as a parameter to predict lethality, is an example of this approach.

In conclusion, the present work collected data and examined low-dose–response models for inhalational anthrax in the rabbit. The CR and MCR models appear to describe spore germination period, overall dose–response and disease incubation period following low-dose exposure quite well. Investigators should continue to advance these models, perhaps by revisiting the monkey model or developing a guinea pig model, to further assess if they can be used to support a low-dose inhalational anthrax risk assessment in man.

Appendix A. Supporting information

Supplementary data associated with this article can be found in the online version at http://dx.doi.org/10.1016/j.jtbi.2013.03.020.

References

Barnes, J.M., 1947. Penicillin and *B. anthracis*. J. Pathol. Bacteriol. 59, 113–125.

Bartrand, T.A., Weir, M.H., Haas, C.N, 2008. Dose–response models for inhalation of *Bacillus anthracis* spores: interspecies comparisons. Risk Anal. 28, 1115–1124.

Bensman, M.D., Mackie, R.S., Minter, Z.A., Gutting, B.W., 2012. Effect of animal sera on *Bacillus anthracis* Sterne spore germination and vegetative cell growth. J. Appl. Microbiol. 113, 276–283.

Brookmeyer, R., Blades, N., 2002. Prevention of inhalational anthrax in the US outbreak. Science 295, 1861.

Brookmeyer, R., Blades, N., Hugh-Jones, M., Henderson, D., 2001. The statistical analysis of truncated data: application to the Sverdlovsk anthrax outbreak. Biostatistics 2, 233–247.

Brookmeyer, R., Johnson, E., Bollinger, R., 2003. Modeling the optimum duration of antibiotic prophylaxis in an anthrax outbreak. PNAS 100, 10129–10132.

Brookmeyer, R., Johnson, E., Barry, S, 2005. Modelling the incubation period of anthrax. Stat. Med. 24, 531–542.

Caipo, M.L., Dufy, S., Zhao, L., Schaffner, D.W., 2002. *Bacillus megaterium* spore germination is influenced by inoculum size 92, 879–884.

Canter, D.A., 2005. Addressing residual risk issues at anthrax cleanups: how clean is safe? J. Toxicol. Environ. Health A 68, 1017–1032.

Coleman, M.E., Thran, B., Morse, S.S., Hugh-Jones, M., Massulik, S., 2008. Inhalation anthrax: dose response and risk analysis,. Biosecur. Bioterror. 6, 147–159.

Day, J., Friedman, A., Schlesinger, L.S., 2011. Modeling the host response to inhalation anthrax. J. Theor. Biol. 276, 199–208.

Dewan, P.K., Fry, A.M., Laserson, K., Tierney, B.C., Quinn, C.P., Hayslett, J.A., Broyles, L.N., Shane, A., Winthrop, K.L., Walks, I., Siegel, L., Hales, T., Semenova, V.A., Romero-Steiner, S., Elie, C., Khabbaz, R., Khan, A.S., Hajjeh, R.A., Schuchat, A., 2002. Inhalational anthrax outbreak among postal workers, Washington, DC. Emerg. Infect. Dis. 8, 1066–1072.

Dixon, T.C., Meselson, M., Guillemin, J., Hanna, P.C., 1999. Anthrax. N. Engl. J. Med. 341, 815–826.

EPA, 2011. Acute low dose *Bacillus anthracis* Ames inhalation exposure in the rabbit, US EPA, Washington, DC, EPA/600/R-11/0075.

Frazier, A.A., Franks, T.J., Galvin, J.R., 2006. Inhalational anthrax. J. Thorac. Imaging 21, 252–258.

Friedlander, A.M., Welkos, S.L., Pitt, M.L.M., Ezzell, J.W., Worsham, P.L., Rose, K.J., Ivins, B.E., Lowe, J.R., Howe, G.B., Mikesell, P, Lawrence, W.B., 1993. Postexposure prophylaxis against experimental inhalation anthrax. J. Infect. Dis. 167, 1239–1242.

Fujiya, M., Musch, M.W., Nakagawa, Y., Hu, S., Alverdy, J., Kohgo, Y., Schneewind, O., Jabri, B., Chang, E.B., 2007. The *Bacillus subtilis* quorum-sensing molecule CSF contributes to intestinal homeostasis via OCTN2, a host cell membrane transporter. Cell Host Microbe 1, 299–308.

Gutting, B., Channel, S., Berger, A., Gearhart, J., Andrews, G., Sherwood, R., Nichols, T., 2008. Mathematically modeling inhalational anthrax. Microbe 3, 78–85.

Gutting, B.W., Gaske, K.S., Schilling, A.S., Slaterbeck, A.F., Sobota, L., Mackie, R.S., Buhr, T.L., 2005. Differential susceptibility of macrophage cell lines to *Bacillus anthracis*—Vollum 1B. Toxicol. In Vitro 19, 221–229.

Gutting, B.W., Nichols, T., Channel, S., Gearhart, J., Andrews, G., Berger, A., Mackie, R., Watson, B., Taft, S., Overheim, K., Sherwood, R., 2012. Rabbit model of inhalational anthrax (Ames strain) with and without vaccination: lung deposition, kinetics of germination/dissemination, and host-inflammatory response following lethal and non-lethal doses. Front. Cell. Inf. Microbiol. 2, 87.

Haas, C., 2002. On the risk of mortality to primates exposed to anthrax spores. Risk Anal. 22, 189–193.

Hambleton, P., Carman, J.A., Melling, J., 1994. Anthrax: the disease in relation to vaccines. Vaccine 2, 125–132.

Henderson, D.W., Peacock, S., Belton, F.C., 1956. Observations on the prophylaxis of experimental pulmonary anthrax in the monkey. J. Hyg. (Lond) 54, 28–36.

Holtz, T.H., Ackelsberg, J., Kool, J.L., Rosselli, R., Marfin, A., Matte, T., Beatrice, S.T., Heller, M.B., Hewett, D., Moskin, L.C., Bunning, M.L., Layton, M., 2003. Isolated case of bioterrorism-related inhalational anthrax, New York City, 2001. Emerg. Infect. Dis. 9, 689–696.

Huang, Y., Haas, C., 2009. Time-dose–response models for microbial risk assessment. Risk Anal. 29, 648–661.

Jernigan, D.B., Raghunathan, P.L., Bell, B.P., Brechner, R., Bresnitz, E.A., Butler, J.C., Cetron, M., Cohen, M., Doyle, T., Fischer, M., Greene, C., Griffith, K.S., Guarner, J., Hadler, J.L., Hayslett, J.A., Meyer, R., Petersen, L.R., Phillips, M., Pinner, R., Popovic, T., Quinn, C.P., Reefhuis, J., Reissman, D., Rosenstein, N., Schuchat, A., Shieh, W.J., Siegal, L., Swerdlow, D.L., Tenover, F.C., Traeger, M., Ward, J.W., Weisfuse, I., Wiersma, S., Yeskey, K., Zaki, S., Ashford, D.A., Perkins, B.A., Ostroff, S., Hughes, J., Fleming, D., Koplan, J.P., Gerberding, J.L., 2002. Investigation of bioterrorism-related anthrax, United States, 2001: epidemiologic findings. Emerg. Infect. Dis. 8, 1019–1028.

Johnson, K., Busta, F.F., 1984. Heat-induced temperature sensitivity of outgrowing *Bacillus cereus* spores. Appl. Environ. Microbiol. 47, 768–774.

Kumar, R., Chow, C.C., Bartels, J.D., Clermont, G., Vodvotz, Y., 2008. A mathematical simulation of the inflammatory response to anthrax infection. Shock 29, 104–111.

Lever, M.W., Stagg, A.J., Nelson, M., Pearce, P., Stevens, D.J., Scott, E.A.M., Simpson, A. J.H., Fulop, M.J., 2008. Experimental respiratory anthrax infection in the common marmoset (*Callithrix jacchus*). Int. J. Exp. Pathol. 89, 171–179.

MacIntyre, C.R., Seccull, A., Lane, J.M., Plant, A., 2006. Development of a risk-priority score for category A bioterrorism agents as an aid for public health policy. Mil. Med. 171, 589–594.

Mock, M., Fouet, A, 2001. Anthrax. Annu. Rev. Microbiol. 55, 647–671.

Pinzon-Areango, P.A., Nagarajan, R., Camesano, T.A., 2010. Effects of L-alanine and inosine germinants of the elasticity of *Bacillus anthracis* spores. Langmuir 26, 6535–6541.

Pitt, M.L., Little, S.F., Ivins, B.E., Fellows, P., Barth, J., Hewetson, J., Gibbs, P., Dertzbaugh, M., Friedlander, A.M., 2001. In vitro correlate of immunity in a rabbit model of inhalational anthrax. Vaccine 19, 4768–4773.

Raber, E., 2011. The challenge of determining the need remediation following a wide-area biological release. Biosecur. Bioterror. 9, 257–261.

Sartwell, P.E., 1950. The distribution of incubation periods of infectious disease. Am. J. Hyg. 51, 310–318.

Twenhafel, N., 2011. Pathology of inhalational anthrax animal models. Vet. Pathol. 47, 819–830.

Watson, A., Keir, D., 1994. Information on which to base assessments of risk from environments contaminated with anthrax spores. Epidemiol. Infect. 113, 479–490.

Welkos, S., Little, S., Friedlander, A., Fritz, D., Fellows, P., 2001. The role of antibodies to *Bacillus anthracis* and anthrax toxin components in inhibiting the early stages of infection by anthrax spores. Microbiology 147, 1677–1685.

Welkos, S., Friedlander, A., Weeks, S., little, S., Mendelson, I., 2002. In-vitro characterization of the phagocytosis and fate of anthrax spores in macrophages and the effects of anti-PA antibody. J. Med. Microbiol. 51, 821–831.

Wilkening, D., 2006. Sverdlovsk revisited: modeling human inhalation anthrax. PNAS 103, 7589–7594.

Wilkening, D., 2008. Modeling the incubation period of inhalational anthrax. Med. Decis. Making 28, 593–605.

Yee, S., Hatkin, J., Dyer, D., Orr, S., Pitt, M., 2010. Aerosolized *Bacillus anthracis* infection in New Zealand white rabbits: natural history and intravenous levofloxacin treatment. Comp. Med. 60, 461–468.

Zaucha, G.M., Pitt, M.L.M., Estep, J., Ivins, B.E., Friedlander, A.M., 1998. The pathology of experimental anthrax in rabbits exposed by inhalation and subcutaneous inoculation. Arch. Pathol. Lab. Med. 122, 982–992.

Zhang, J., et al., 2011. Quantitative analysis of spatial-temporal correlations during germination of spores of *Bacillus* species. J. Bacteriol. 193, 3765–3772.